

# A STATE TRANSITION OF GX 339–4 OBSERVED WITH THE *ROSSI X-RAY TIMING EXPLORER*

T. BELLONI,<sup>1,2</sup> M. MÉNDEZ,<sup>1,3</sup> M. VAN DER KLIS,<sup>1</sup> W. H. G. LEWIN,<sup>4</sup> AND S. DIETERS<sup>5</sup>

*Received 1999 April 27; accepted 1999 May 10; published 1999 June 16*

## ABSTRACT

We report the results of observations with the *Rossi X-ray Timing Explorer* of the black hole candidate GX 339–4 during the state transition of 1998. We find that both the X-ray spectrum and the characteristics of the time variability after the transition are typical of a high/soft state. We cannot exclude that the source went through an intermediate state before entering the high state. We discuss the results and compare them with other known black hole candidates.

*Subject headings:* accretion, accretion disks — binaries: close — stars: individual (GX 339–4) — X-rays: stars

## 1. INTRODUCTION

GX 339–4 was discovered with the *OSO 7* satellite (Markert et al. 1973) and identified with a  $V \sim 18$  mag star in the optical (Doxsey et al. 1979), with an  $\sim 15$  hr photometric period interpreted as the orbital period (Callanan et al. 1992). Although no dynamical measurement of the mass of the compact object is available, the source is included in the class of black hole candidates because of its fast aperiodic variability and the occurrence of spectral/timing transitions similar to those of established sources in the class (see Méndez & van der Klis 1997). The source is usually observed in the low state (LS), where the 1–10 keV energy spectrum is a power law with a spectral index of  $\Gamma \sim 1.5$ –2.0 (Tananbaum et al. 1972) and the power spectrum consists of a strong (25%–50% fractional rms) band-limited noise component similar to that observed in Cygnus X-1 (Oda et al. 1971; Miyamoto et al. 1992). In the high state (HS), the source is brighter below 10 keV, and an ultrasoft component appears in the energy spectrum, while the power-law component steepens considerably; the power spectrum is reduced to a power law with a few percent fractional rms (Grebenev et al. 1991). In the very high state (VHS), observed on only one occasion, the source is much brighter below 10 keV, mainly because of the increased luminosity of the ultrasoft thermal component; the power law has a photon index of  $\Gamma \sim 2.5$ ; and the power spectrum shows a 1%–15% rms variable band-limited noise with a characteristic break frequency much higher than in the LS (Miyamoto et al. 1991). Méndez & van der Klis (1997) identified a fourth state in GX 339–4, called the intermediate state (IS), observed also in GS 1124–68 by Belloni et al. (1997): its timing and spectral characteristics are similar to those of the VHS, but the IS appears at much lower luminosities than the VHS. In GS 1124–68, as the outburst proceeded, the source moved from the VHS to the HS to the IS and then to the LS, indicating that the IS and VHS are indeed different states (see Belloni et al. 1997). Currently, GX 339–4 is the only system, together

with GS 1124–68, in which all four states have been observed, although recently the superluminal transient GRO J1655–40 has shown similar behavior (Méndez, Belloni, & van der Klis 1998).

In this Letter, we report the results of the *Rossi X-ray Timing Explorer* (*RXTE*)/Proportional Counter Array (PCA) observations of GX 339–4 during a transition to the HS in 1998 and compare them with previous observations in the LS (analyzed in detail by Nowak, Wilms, & Dove 1999 and Wilms et al. 1999).

## 2. X-RAY OBSERVATIONS

### 2.1. All-Sky Monitor

The All-Sky Monitor (ASM; Levine et al. 1996) on board the *RXTE* observed GX 339–4 almost continuously since the beginning of the mission. The ASM light curve, in 1 day bins, is shown in Figure 1. The source was in a low-flux, hard state for the whole of 1996 and 1997. The flux level and the hardness ratio during this period indicate that the source was in the low state. Some variability can be seen, in the form of little “outbursts,” whose ASM flux is anticorrelated with the hard X-ray flux as observed by the *Compton Gamma-Ray Observatory* (*CGRO*)/BATSE (see Rubin et al. 1998). In the beginning of 1998 January, a sharp increase in the ASM count rate is visible. The source reached a level of approximately 20 counts  $s^{-1}$  and remained approximately constant for  $\sim 150$  days before the flux started to decrease, until it finally went back to a low value (around  $\sim 2$  counts  $s^{-1}$ ). The switch to a higher count rate triggered a target-of-opportunity (TOO) observation with the PCA/High-Energy X-ray Timing Experiment (HEXTE) instruments.

### 2.2. PCA/HEXTE

In response to the TOO call, the *RXTE* observed GX 339–4 for 45 ks between 1998 January 15 and 18 (observation B; see Table 1). The time of the observations corresponds to the rise phase of the outburst, just after a small flare (see Fig. 1). A month later, the source reached the peak of the outburst (Fig. 1), and a second, much shorter pointing was performed (observation C; see Table 1). In addition, we analyzed a much older pointing that was extracted from the *RXTE* archive (observation A; see Table 1), obtained when the source was in the LS (Fig. 1).

From PCA observations A and B, we divided the light curve from the high-time resolution data in segments, produced a power spectrum from each segment, and averaged them to-

<sup>1</sup> Astronomical Institute “Anton Pannekoek,” University of Amsterdam and Center for High-Energy Astrophysics, Kruislaan 403, Amsterdam, SJ, NL-1098, Netherlands.

<sup>2</sup> Present address: Osservatorio Astronomico di Brera, via E. Bianchi 46, Merate, I-23807, Italy.

<sup>3</sup> Facultad de Ciencias Astronómicas y Geofísicas, Universidad Nacional de La Plata, Paseo del Bosque S/N, 1900 La Plata, Argentina.

<sup>4</sup> Massachusetts Institute of Technology, Center for Space Research, 70 Vassar Street, Room 37-627, Cambridge, MA 02139.

<sup>5</sup> Center for Space Plasma and Aeronomic Research, University of Alabama in Huntsville, Huntsville, AL 35899.

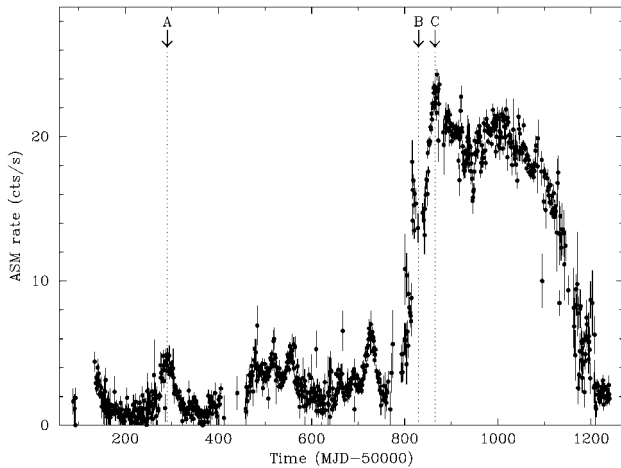


FIG. 1.—*RXTE*/ASM light curve of GX 339–4. The bin size is 1 day. The arrows and the dotted lines indicate the times of the three pointed observations discussed in the text.

gether. The length of each segment was 256 and 64 s for observations A and B, respectively. All PCA channels were included in the analysis. We subtracted from the resulting power spectra the contribution from the Poissonian noise and the very large event window contribution (Zhang et al. 1995). Because of its shortness, no useful data could be obtained from observation C. The two power spectra can be seen in Figure 2.

Observation A looks like a typical LS, with a strong band-limited noise component. We fitted this power spectrum with a rather complicated model, consisting of a broken power law, a zero-centered Lorentzian of width  $\nu_0 = 0.75 \pm 0.04$  Hz, and a narrow QPO at  $\nu_1 = 0.35 \pm 0.03$  Hz. In addition, a second QPO at  $\nu_2 = 0.48 \pm 0.03$  Hz (visible as a relatively small but significant feature in Fig. 2) and a broad Lorentzian bump at  $\nu_3 = 3.14 \pm 0.17$  Hz were needed. An examination of more LS power spectra from other observations showed that  $\nu_1$  and  $\nu_2$  are probably the second and third harmonics of a fundamental  $\nu_0 \sim 0.16$  Hz. The total fractional rms in the 0.01–100 Hz range is 41%. The model used is different from that of the much more complete work on the LS by Nowak et al. (1999), but we use this observation only for comparison. The power spectrum from observation B looks completely different. Not much noise is observed, and a simple power-law model (with an index of  $0.62 \pm 0.04$ ) gives a good fit to the data. The total rms in the 0.1–100 Hz band is 2%. This weak noise component is characteristic of the HS.

From all three observations, after checking that there were no large flux variations, we extracted PCA and HEXTE energy spectra following the standard procedures for *XTE*, using FTOOLS 4.2. For spectral accumulation, we selected intervals where all five PCA detectors were turned on and the pointing offset was less than  $0^\circ.02$ . In order to minimize contamination, we further selected data only from intervals when the Earth elevation angle of the source was greater than  $10^\circ$  and the satellite was well outside the South Atlantic Anomaly. PCA background files were produced with the program PCABACKEST version 2.1b. We produced PCA detector response matrices using PCARMF v3.5. For the HEXTE, we accumulated background spectra from off-source pointings, and we used the latest background matrices made available by the *RXTE* team. For observations B and C, not enough signal was present in the HEXTE data above the first few channels, and

TABLE 1  
PCA/HEXTE OBSERVATION LOG

Observation	Start (UT)	End (UT)	PCA Exposure (s)
A .....	1996 Jul 26 (18:20)	1996 Jul 26 (20:15)	5200
B .....	1998 Jan 15 (03:56)	1998 Jan 18 (03:20)	45400
C .....	1998 Feb 21 (15:04)	1998 Feb 21 (15:36)	1600

those were therefore not used in the analysis. We used the HEXTE detector response matrices from 1997 March 20. For the spectral fits, we used XSPEC 10.00 and added a 1% systematic error to the PCA spectra.

We fitted the spectra with a rather complex but standard model, consisting of a power law with an exponential cutoff at high energies, a multicolor disk blackbody (Mitsuda et al. 1984), and a Gaussian emission line. Correction for interstellar absorption was included as well as a “smeared edge” (Ebisawa et al. 1994) that was found to be needed in order to obtain a satisfactory fit. The central energy of the Gaussian line was kept fixed at 6.4 keV. Not all components were needed to model all spectra. No Gaussian line and no disk-blackbody components were needed for observation A, and no smeared edge was needed for observation C (in this case, because of the short exposure time). Notice that, for the HS spectra, the emission line and the edge could arise from the fact that the continuum model is an approximation, since here the thermal component is strong. Indeed, both the line and the edge are located in the energy range where the two continuum components become comparable. We do not attempt a physical interpretation of these features. The best-fit parameters can be found in Table 2. The spectra and the residuals after model subtraction are shown in Figure 3. It is evident from Table 2 that the large increase in X-ray flux between observations B/C and observation A is due entirely to the appearance of a soft thermal component, while the power-law component steepens and becomes fainter.

### 3. DISCUSSION

The *RXTE*/ASM light curve shown in Figure 1 strongly suggests that GX 339–4 underwent a transition from the LS to the HS. The long-term behavior consists basically of an interval of  $\sim 400$  days of increased ASM flux. Our power spectra and

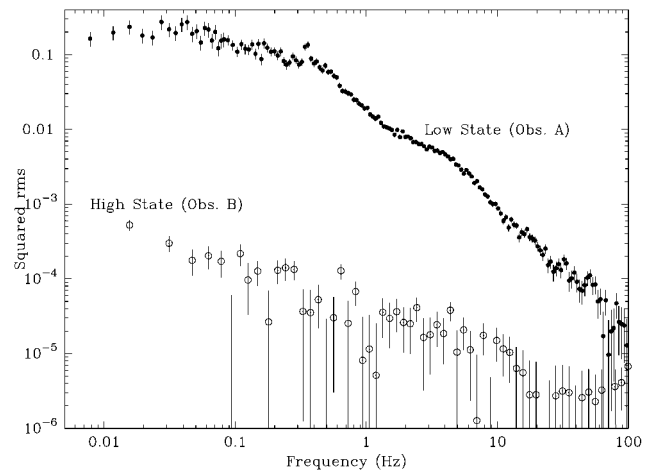


FIG. 2.—Power spectra from observations A (filled circles) and B (open circles).

energy spectra are unambiguous: during observation A (reported also by other authors; see, e.g., Nowak et al. 1999 and Wilms et al. 1999), the source was in its low state, the state in which GX 339–4 is mostly observed. This is characterized by a flat ( $\Gamma \sim 1.6$ ) power-law energy spectrum (with evidence of a high-energy cutoff) and by a strong band-limited noise in the power spectrum with a QPO peak and its harmonics. At 4 kpc (see Zdziarski et al. 1998), the 2.5–20 keV observed luminosity is  $\sim 4 \times 10^{36}$  ergs s $^{-1}$ . Both the energy distribution and the power spectrum are extremely similar to those of Cyg X-1. This similarity includes the  $\sim 3$  Hz broad bump detected in the power spectrum. Notice that the low-frequency QPO at 0.35 Hz and the 3 Hz bump have been shown by Psaltis, Belloni, & van der Klis (1999) to fit a correlation that is observed when combining QPO data from a number of sources, both contain neutron star systems and black hole candidates.

The X-ray properties of the source changed drastically after the transition (observations B and C). Very little variability is observed in the timing domain: the power spectrum shows only a weak power-law component. The energy spectrum is dominated by a thermal component, which we fitted with the standard model used for black hole candidates, i.e., a multicolor disk blackbody: the output parameters are the temperature of the inner edge of the accretion disk and the radius of the inner edge itself. Interestingly, the radius that we derive is in the range expected for the innermost stable orbit around a black hole, although the precise value cannot be determined since we do not know the inclination of the system. Moreover, note that due to the approximated form of the disk-blackbody model used (see Mitsuda et al. 1984), the derived radius is likely to be smaller than the real one since the effective blackbody temperature is probably smaller than the observed color temperature (Lewin, van Paradijs, & Taam 1995). The 2.5–20 keV luminosity of this component (at a distance of 4 kpc) is  $5 \times 10^{36}$  and  $8 \times 10^{36}$  ergs s $^{-1}$  for observation B and C, respectively, whereas the corresponding luminosity of the (steeper) power-law component is 10 and  $4 \times 10^{35}$  ergs s $^{-2}$ , respectively. The difference between the two pointings indicates a further anticorrelation between the two components. These parameters are very similar to what is observed for the HS both in GX 339–4 itself and in other sources (GX 339–4 [Grebenev et al. 1991]; GS 1124–68 [Ebisawa et al. 1994]; GRO J1655–40 [Méndez et al. 1998]; 4U 1630–47 [Kuulkers et al. 1998 and Oosterbroek et al. 1998]; LMC X-3 [Ebisawa et al. 1993]). Interestingly, Fender et al. (1999) found an anticorrelation between the X-ray flux (from the *RXTE*/ASM) and the radio flux. They show that the radio flux is strongly suppressed during the HS period. This is analogous to what is observed in Cyg X-1, where there is a suppression of radio flux during transitions to and from a LS (see Zhang et al. 1997b). The transition is clearly detected by the *CGRO*/BATSE, in the form of an anticorrelation with the ASM data (Fender et al. 1999).

Comparing our results with those of Cui et al. (1997a, 1997b), we can see that, despite the similarity in long-term light curves, in Cyg X-1 the situation is different. During the transition, a bright, soft component appears in the energy spectrum of Cyg X-1, but the power-law component remains relatively strong. Moreover, the power spectra show either a band-limited noise component or a power-law component, but always with a fractional rms well above 10%. This is also evident in the light curve in Figure 1 from Cui et al. (1997a), where large variations can be seen. Following Belloni et al. (1996), comparing our results for GX 339–4, we confirm that Cyg X-1

during the transition of 1996 never reached the HS (as observed in other sources like LMC X-3, which is always seen in this state; Ebisawa et al. 1993) but switched from the LS to the IS and back. However, there is no sign of the IS in our observations. Méndez & van der Klis (1997) compiled a list of flux thresholds for the various states based on previous state transitions. From their list, assuming a typical HS energy spectrum, we estimate that, based on the previous transitions, the HS should not have started until a count rate of  $\sim 30$  counts s $^{-1}$  had been reached in the *RXTE*/ASM. If GX 339–4 went into the IS before our observations, it did it at a different flux level. As a direct comparison, the IS in Méndez & van der Klis had a 2–10 keV flux of  $1.5 \times 10^{-9}$  ergs cm $^{-2}$  s $^{-1}$ , a factor of 2.3 less than what we observe here. Notice that just before our

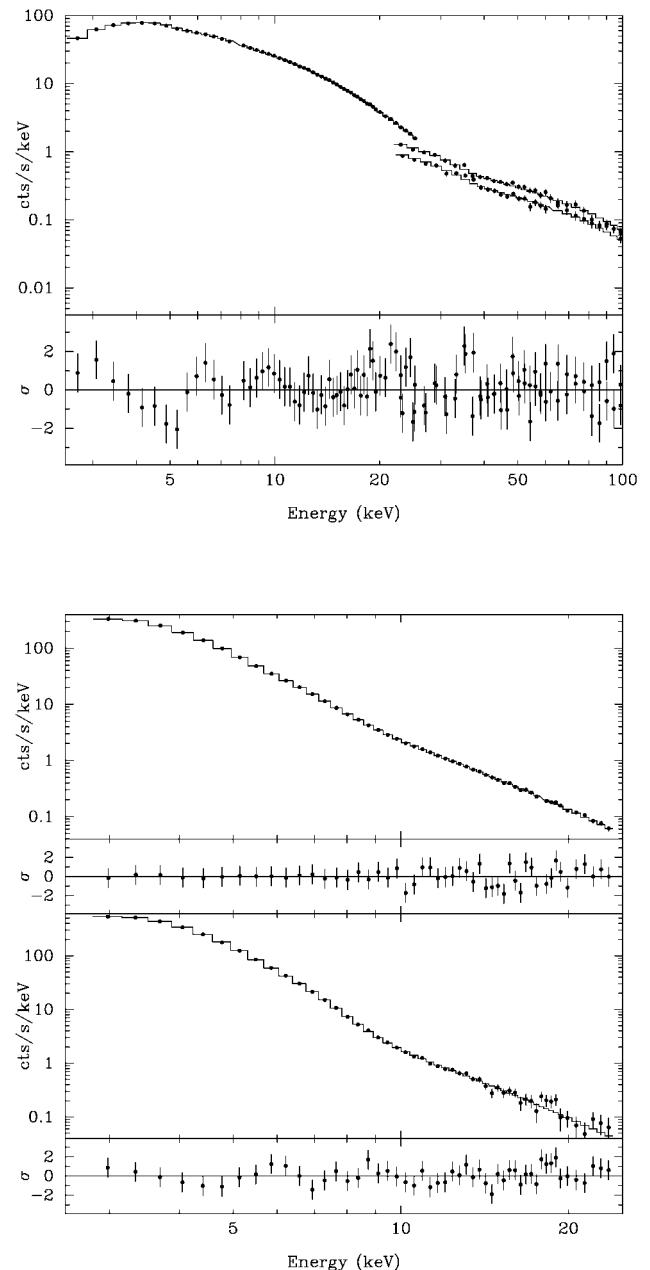


FIG. 3.—Energy spectra from observations A (top panel) and B/C (bottom panel). The residuals after subtraction of the best-fit models described in the text are shown.

TABLE 2  
BEST-FIT PARAMETERS FOR ENERGY SPECTRA FROM THREE OBSERVATIONS OF  
GX 339-4 WITH MODEL DESCRIBED IN TEXT

PARAMETERS	OBSERVATION		
	A	B	C
$N_H$ (cm $^{-2}$ )	$(1.1 \pm 0.1) \times 10^{21}$	$<9.7 \times 10^{21}$	$<2.0 \times 10^{21}$
$\Gamma$	$1.63 \pm 0.01$	$2.57 \pm 0.05$	$2.12 \pm 0.19$
$E_{\text{cut}}$ (keV)	$270 \pm 60$	...	...
$F_{\text{pl}}$ (ergs cm $^{-2}$ s $^{-1}$ )	$2.3 \times 10^{-9}$	$6.2 \times 10^{-10}$	$2.0 \times 10^{-10}$
$kT$ (keV)	...	$0.63 \pm 0.01$	$0.72 \pm 0.01$
$R_{\text{in}} (\cos i)^{1/2}$ (km)	...	$28.7 \pm 4.0$	$25.4 \pm 0.6$
$F_{\text{dbb}}$ (ergs cm $^{-2}$ s $^{-1}$ )	...	$2.5 \times 10^{-9}$	$4.6 \times 10^{-9}$
$E_{\text{lin}}$ (keV)	...	6.4 (FIX)	6.4 (FIX)
$\sigma_{\text{lin}}$ (keV)	...	$1.45 \pm 0.14$	$0.79 \pm 0.10$
$EW_{\text{lin}}$ (eV)	...	350	319
$E_{\text{edg}}$ (keV)	$7.26 \pm 0.24$	$6.69 \pm 0.15$	...
$\tau_{\text{edg}}$	$0.67 \pm 0.24$	$>6.2$	...
$W_{\text{edg}}$ (keV)	$4.79 \pm 2.02$	$16.8 \pm 5.4$	...
$\chi_r^2$ (dof)	0.94 (146)	0.83 (41)	0.88 (46)

NOTE.—Errors are 1  $\sigma$ . Fluxes are in the 2.5–20.0 keV band. The inner disk radius is computed assuming a distance of 4 kpc. FIX means that the parameter was fixed to that value.

observation B, a small peak is visible in Figure 1, at 15–18 ASM counts s $^{-1}$ . It is possible that during this time, the source indeed went through an IS, although we cannot confirm it. This indicates that, if flux is a good tracer of accretion rate, it is not the only parameter governing these transitions.

A simple classification in terms of four basic states with a definite dependence on flux (see van der Klis 1995 for a review) fails to reproduce the whole wealth of behaviors observed in black hole candidates. In addition to sources that do not seem to follow the simple scheme outlined above (e.g., GRS 1915+105 [Belloni 1998]; XTE J1550-564 [Sobczak et al. 1999]; GS 2023+338 [Zycki, Done, & Smith 1999]), there are other examples indicating that the accretion rate is not the only parameter governing these transitions. This is particularly clear in the case of the 1998 outburst of 4U 1630-47, where a transition between the IS and the HS was not followed by a reverse transition as the source went back into quiescence (Dieters et al. 1999). Moreover, in 1996, the *RXTE* observed a state transition of Cyg X-1; the source increased its soft X-ray flux by a factor of 3–4 (Cui 1996; Cui, Focke, & Swank 1996), while the bolometric flux remained approximately constant (Zhang et al. 1997a).

The results presented in this Letter, together with the

recent results for 4U 1630-47 and other transients like GRS 1915+105 (Belloni 1998), GRO J1655-40 (Méndez et al. 1998; Tomsick et al. 1999), XTE J1550-564 (Cui et al. 1999; Sobczak et al. 1999), and XTE J1748-288 (Revnivtsev, Trudolyubov, & Borozdin 1999; Focke & Swank 1999) show that the classification in terms of the four source states is followed faithfully by some sources (like GRO J1655-40, XTE J1550-564, and XTE J1748-288) but is complicated by the absence of a unique flux “trigger” for transitions between states (like in 4U 1630-47 and GX 339-4) and by completely different behavior in the case of GRS 1915+105.

M. M. is a fellow of the Consejo Nacional de Investigaciones Científicas y Técnicas de la República Argentina. This work was supported in part by the Netherlands Foundation for Research in Astronomy (ASTRON) under grant 781-76-017. T. B. is supported by NWO Spinoza grant 08-0 to E. P. J. van den Heuvel. S. D. is supported by NASA LTSA grant NAG5-6021. W. H. G. L. acknowledges support from NASA. This research has made use of data obtained through the High Energy Astrophysics Science Archive Research Center Online Service, provided by the NASA/Goddard Space Flight Center.

#### REFERENCES

- Belloni, T. 1998, *NewA*, 42, 585  
 Belloni, T., Méndez, M., van der Klis, M., Hasinger, G., Lewin, W. H. G., & van Paradijs, J. 1996, *ApJ*, 472, L107  
 Belloni, T., van der Klis, M., Lewin, W. H. G., van Paradijs, J., Dotani, T., Mitsuda, K., & Miyamoto, S. 1997, *A&A*, 322, 857  
 Callanan, P. J., Charles, P. A., Honey, W. B., & Thorstensen, J. R. 1992, *MNRAS*, 255, 395  
 Cui, W. 1996, *IAU Circ.* 6404  
 Cui, W., Focke, W., & Swank, J. 1996, *IAU Circ.* 6439  
 Cui, W., Heindl, W. A., Rothschild, R. E., Zhang, S. N., Jahoda, K., & Focke, W. 1997a, *ApJ*, 474, L57  
 Cui, W., Zhang, S. N., Chen, W., & Morgan, E. H. 1999, *ApJ*, 512, L43  
 Cui, W., Zhang, S. N., Focke, W., & Swank, J. H. 1997b, *ApJ*, 484, 383  
 Dieters, S., et al. 1999, in preparation  
 Doxsey, R., Grindlay, J., Griffiths, R., Bradt, H., Johnston, M., Leach, R., Schwartz, D., & Schwartz, J. 1979, *ApJ*, 228, L67  
 Ebisawa, K., Makino, F., Mitsuda, K., Belloni, T., Cowley, A. P., Schmidtke, P. C., & Treves, A. 1993, *ApJ*, 403, 684  
 Ebisawa, K., et al. 1994, *PASJ*, 46, 375  
 Fender, R., et al. 1999, *ApJ*, 519, L165  
 Focke, W. B., & Swank, J. H. 1999, in preparation  
 Grebenev, S. A., Sunyaev, R. A., Pavlinskii, M. N., & Dekhanov, I. A. 1991, *Soviet Astron. Lett.*, 17, 413  
 Kuulkers, E., Wijnands, R., Belloni, T., Méndez, M., van der Klis, M., & van Paradijs, J. 1998, *ApJ*, 494, 753  
 Levine, A. M., Bradt, H., Cui, W., Jernigan, J. G., Morgan, E. H., Remillard, R. A., Shirey, R., & Smith, D. 1996, *ApJ*, 469, L33  
 Lewin, W. H. G., van Paradijs, J., & Taam, R. E. 1995, in *X-Ray Binaries*, ed W. H. G. Lewin, J. van Paradijs, & E. van den Heuvel (Cambridge: Cambridge Univ. Press), 175  
 Markert, T. H., Canizares, C. R., Clark, G. W., Lewin, W. H. G., Schnopper, H. W., & Sprott, G. F. 1973, *ApJ*, 184, L67  
 Méndez, M., Belloni, T., & van der Klis, M. 1998, *ApJ*, 499, L187  
 Méndez, M., & van der Klis, M. 1997, *ApJ*, 479, 926  
 Mitsuda, K., et al. 1984, *PASJ*, 36, 741  
 Miyamoto, S., Kimura, K., Kitamoto, S., Dotani, T., & Ebisawa, K. 1991, *ApJ*, 383, 784  
 Miyamoto, S., Kitamoto, S., Iga, S., Negoro, H., & Terada, K. 1992, *ApJ*, 391, L21  
 Nowak, M. A., Wilms, J., & Dove, J. B. 1999, *ApJ*, 517, 355

- Oda, M., Gorenstein, P., Gursky, H., Kellogg, E., Schreier, E., Tananbaum, H., & Giacconi, R. 1971, *ApJ*, 166, L1
- Oosterbroek, T., Parmar, A. N., Kuulkers, E., Belloni, T., van der Klis, M., Frontera, F., & Santangelo, A. 1998, *A&A*, 340, 431
- Psaltis, D., Belloni, T., & van der Klis, M. 1999, *ApJ*, in press
- Revnivtsev, M. G., Trudolyubov, S. P. & Borozdin, K. N. 1999, *MNRAS*, submitted
- Rubin, B. C., Harmon, B. A., Paciesas, W. S., Robinson, C. R., Zhang, S. N., & Fishman, G. J. 1998, *ApJ*, 492, L67
- Sobczak, G. J., McClintock, J. E., Remillard, R. A., Levine, A. M., Morgan, E. H., Bailyn, C. D., & Orosz, J. A. 1999, *ApJL*, in press
- Tananbaum, H., Gursky, H., Kellogg, E., Giacconi, R., & Jones, C. 1972, *ApJ*, 177, L5
- Tomsick, J. A., Kaaret, P., Kroeger, R. A., & Remillard, R. A. 1999, *ApJ*, 512, 892
- van der Klis, M. 1995, in *X-Ray Binaries*, ed W. H. G. Lewin, J. van Paradijs, & E. van den Heuvel (Cambridge: Cambridge Univ. Press), 252
- Wilms, J., Nowak, M. A., Dove, J. B., Fender, R. P., & Di Matteo, T. 1999, *ApJ*, in press
- Zdziarski, A. A., Poutanen, J., Mikolajewska, J., Gierlinski, M., Ebisawa, K., & Johnson, W. N. 1998, *MNRAS*, 301, 435
- Zhang, S. N., Cui, W., Harmon, B. A., Paciesas, W. S., Remillard, R. E., & van Paradijs, J. 1997a, *ApJ*, 477, L95
- Zhang, S. N., Mirabel, I. F., Harmon, B. A., Kroeger, R. A., Rodríguez, L. F., Hjellming, R. M., & Rupen, M. P. 1997b, in *AIP Conf. Proc. 410, Fourth Compton Symp.*, ed. C. D. Dermer, M. S. Strickman, & J. D. Kurfess (New York: AIP), 141
- Zhang, W., Jahoda, K., Swank, J. H., Morgan, E. H., & Giles, A. B. 1995, *ApJ*, 449, 930
- Zycki, P. T., Done, C., & Smith, D. A. 1999, *MNRAS*, in press